

Exact analysis of the two-dimensional asymmetric simple exclusion process with attachment and detachment of particles

Yuki Ishiguro^{1,2}, Jun Sato¹

¹Faculty of Engineering, Tokyo Polytechnic University, 5-45-1 Iiyama-minami, Atsugi, Kanagawa 243-0297, Japan

²The Institute for Solid State Physics, The University of Tokyo, 5-1-5 Kashiwanoha, Kashiwa, Chiba 277-8581, Japan

Abstract. The asymmetric simple exclusion process (ASEP) is a paradigmatic driven-diffusive system that describes the asymmetric diffusion of particles with hardcore interactions in a lattice. Although the ASEP is known as an exactly solvable model, most exact results are limited to one-dimensional systems. Recently, the exact steady state in the multi-dimensional ASEP has been proposed [1]. The research focused on the situation where the number of particles is conserved. In this paper, we consider the two-dimensional ASEP with the attachment and detachment of particles (ASEP-LK), where particle number conservation is violated. By employing the result in Ref. [1], we construct the exact steady state of the ASEP-LK and reveal its properties through the exact computation of physical quantities.

1. Introduction

Driven-diffusive systems play a central role in exploring the physics of nonequilibrium systems. A variety of complex nonequilibrium phenomena, such as biological transport [2, 3] and traffic flow [4, 5], can be modeled by driven-diffusive systems. Among them, the asymmetric simple exclusion process (ASEP) is actively studied as a fundamental model for describing nonequilibrium transportation phenomena [2–33]. The ASEP is a stochastic process describing the asymmetric diffusion of particles with hardcore interactions in a lattice. Although the model is simple, it contains rich nonequilibrium physics, including boundary-induced phase transitions [8] and the KPZ universality class [32, 33]. In addition, the ASEP is an exactly solvable model and has attracted attention in the context of mathematical physics [6–30]. In the one-dimensional (1D) case, we can evaluate the physical quantities exactly by using appropriate methods, such as the matrix product ansatz [6–10] and the Bethe ansatz [11–28]. However, most of the studies on the exact analysis have been focused on 1D systems, and the exact results of systems beyond one dimension are limited to specific situations [34–41].

Recently, the exact steady states of the ASEP in arbitrary dimensions have been proposed [1]. Although the study has presented the crucial concept for constructing

the solutions of exactly solvable models in more than one dimension, it focused on the situation where the number of particles is conserved. However, many complex nonequilibrium phenomena are often modeled as open systems where particles flow into and out of the system from the environment. Extending the theory to the situation where particle number conservation is violated is important for understanding more diverse nonequilibrium phenomena.

Various extensions of the ASEP have been devised to describe a range of phenomena. The ASEP with Langmuir kinetics (ASEP-LK) is one of the representative extensions [42–50]. In the model, the ASEP is extended by introducing the attachment and detachment of particles in the bulk (Langmuir kinetics), which violates particle number conservation even in periodic and closed boundary conditions. The schematic drawing of the 2D ASEP-LK is shown in Fig. 1. In the 1D case, the exact steady state is constructed under the periodic boundary conditions [45, 46], and that in infinitesimal Langmuir kinetics is conjectured under closed boundary conditions [47]. As a study of the ASEP-LK in a 2D lattice, there are researches that extend it to multi-lane systems [48–50]. However, in the 2D case, the ASEP-LK is mainly investigated through the mean-field approach, and exact results have not been obtained.

In this paper, we construct the exact steady states of the 2D ASEP-LK and reveal their properties based on the exact analysis of physical quantities. We focus on three types of boundary conditions: torus, closed, and multi-lane boundary conditions. In the torus (closed) boundary conditions, we consider the periodic (closed) boundary conditions both in x - and y -directions. In the multi-lane boundary conditions, we consider the closed boundary conditions in x -direction and the periodic boundary conditions in y -direction. By employing the exact results for the standard 2D ASEP without Langmuir kinetics [1], we construct the exact steady state of the ASEP-LK in the periodic boundary conditions and that in the infinitesimal Langmuir kinetics in the closed and multi-lane boundary conditions. Based on the results, we clarify the effect of Langmuir kinetics and two-dimensionality on the properties of the steady state through the computation of physical quantities.

This paper is organized as follows. In Sec. 2, we introduce the 2D ASEP-LK. The model is a continuous-time Markov process, and its time evolution is described by the master equation. In Sec. 3, we focus on the steady state, which is the eigenstate of the Markov matrix with zero eigenvalue. Here, we derive the general expression for the steady state of the ASEP-LK. In Sec. 4, we construct the exact steady state of the ASEP-LK in the periodic boundary conditions and investigate physical quantities. In Sec. 5, we obtain the exact expression of the steady state in infinitesimal Langmuir kinetics under the closed boundary conditions. Through the exact analysis, we reveal the behavior of the density distribution in response to the attachment and detachment ratio. In Sec. 6, we present the exact expression of the steady state in infinitesimal Langmuir kinetics under the multi-lane boundary conditions. Through the exact analysis, we elucidate the effect of the two-dimensionality on the quasi-one-dimensional flow. In Sec. 7, we conclude our results.

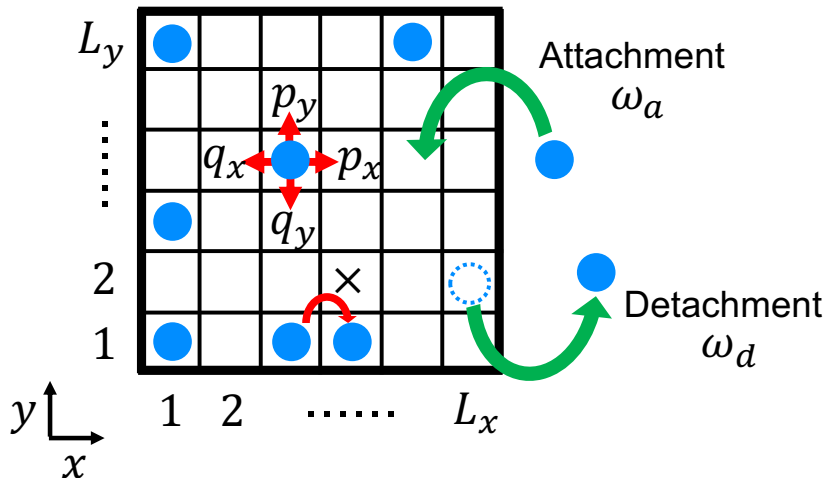


Figure 1. Asymmetric simple exclusion process with Langmuir kinetics (ASEP-LK) in a two-dimensional lattice.

2. Model

2.1. ASEP

The ASEP is a continuous-time Markov process in which hardcore particles hop asymmetrically in a lattice [2–33]. In this paper, we focus on a 2D lattice with a system size $L_T = L_x \times L_y$ (Fig. 1). The updating rule is given as follows. Particles hop to the forward site in the x -direction (y -direction) with a hopping rate p_x (p_y) and to the backward site with a hopping rate q_x (q_y). Due to the hardcore interactions, each site contains at most one particle. We consider the combination of two types of boundary conditions: closed boundary conditions and periodic boundary conditions. When we consider the closed boundary conditions in the x -direction, a particle at site $(x, y) = (L_x, y)$ ($(x, y) = (1, y)$) cannot hop to the forward (backward) direction. In contrast, when we consider the periodic boundary conditions, a particle at site $(x, y) = (L_x, y)$ ($(x, y) = (1, y)$) can hop to the site $(x, y) = (1, y)$ ($(x, y) = (L_x, y)$) with the rate p_x (q_x). In this paper, we consider the three patterns of the combination of boundary conditions: torus, closed, and multi-lane boundary conditions. In the torus (closed) boundary conditions, we consider the periodic (closed) boundary conditions both in the x - and y -direction. In contrast, in the multi-lane boundary conditions, we consider the closed boundary conditions in the x -direction and the periodic boundary conditions in the y -direction. In these boundary conditions, the number of particles N is conserved throughout the time evolution.

The state of a site $\mathbf{r} = (x, y)$ is represented by a Boolean number $n_{\mathbf{r}}$, which is set to $n_{\mathbf{r}} = 0$ ($n_{\mathbf{r}} = 1$) when the site is empty (occupied). A configuration of the ASEP, which is denoted by n , is described by a series of the Boolean numbers $n = (n_{(1,1)}, n_{(2,1)}, \dots, n_{(L_x, L_y)})$. We denote the probability of the system being in a configuration n at time t as $P(n, t)$. The time evolution of $P(n, t)$ is described by the

following master equation:

$$\frac{d}{dt}P(n, t) = \sum_{n' \neq n} [P(n', t)W_h(n' \rightarrow n) - P(n, t)W_h(n \rightarrow n')], \quad (1)$$

where $W_h(n \rightarrow n')$ denotes a transition rate from n to n' through a hopping process.

It is also useful to rewrite the master equation (1) in vector form. The state of a site \mathbf{r} is represented by a two-dimensional vector $|n_{\mathbf{r}}\rangle$, which equals to $|0\rangle$ ($|1\rangle$) when the site is empty (occupied). The L_T -fold tensor product $|n\rangle = \bigotimes_{x=1}^{L_x} \bigotimes_{y=1}^{L_y} |n_{\mathbf{r}}\rangle$ forms an orthonormal basis of the configuration space under normalization. A stochastic state vector is given by

$$|P(t)\rangle = \sum_n P(n, t)|n\rangle. \quad (2)$$

In the Markov process, the expectation value of a physical quantity \hat{A} , which takes a value $A(n)$ in a configuration n , in a state $|P(t)\rangle$ is given by

$$\begin{aligned} \langle \hat{A} \rangle &= \langle \mathcal{P} | \hat{A} | P(t) \rangle \\ &= \sum_n P(n, t) A(n) \end{aligned} \quad (3)$$

where $\langle \mathcal{P} |$ is the projection state defined as

$$\langle \mathcal{P} | := \sum_n \langle n |. \quad (4)$$

The time evolution of $|P(t)\rangle$ is described by the master equation

$$\frac{d}{dt}|P(t)\rangle = \mathcal{H}_{\text{ASEP}}|P(t)\rangle, \quad (5)$$

where the Markov matrix $\mathcal{H}_{\text{ASEP}}$ is given by

$$\begin{aligned} \mathcal{H}_{\text{ASEP}} &= \sum_{i \in \{x, y\}} \sum_{x, y} \left[p_i \left\{ \hat{S}_{\mathbf{r}}^+ \hat{S}_{\mathbf{r}+\mathbf{e}_i}^- - \hat{n}_{\mathbf{r}} (1 - \hat{n}_{\mathbf{r}+\mathbf{e}_i}) \right\} + q_i \left\{ \hat{S}_{\mathbf{r}}^- \hat{S}_{\mathbf{r}+\mathbf{e}_i}^+ - (1 - \hat{n}_{\mathbf{r}}) \hat{n}_{\mathbf{r}+\mathbf{e}_i} \right\} \right] \\ &= \sum_{i \in \{x, y\}} \sum_{x, y} \mathcal{M}_{\mathbf{r}, \mathbf{r}+\mathbf{e}_i}. \end{aligned} \quad (6)$$

Here, the subscripts of operators indicate the sites where the operators act nontrivially, and \mathbf{e}_i represents the unit vector in i -direction. We introduce the half of the Pauli matrices $\hat{S}_{\mathbf{r}}^{x, y, z}$, the ladder operators $\hat{S}_{\mathbf{r}}^{\pm} = \hat{S}_{\mathbf{r}}^x \pm i \hat{S}_{\mathbf{r}}^y$, the number operators $\hat{n}_{\mathbf{r}} = 1/2 - \hat{S}_{\mathbf{r}}^z$, and the local Markov matrix

$$\mathcal{M}_{\mathbf{r}, \mathbf{r}+\mathbf{e}_i} = \begin{pmatrix} 0 & 0 & 0 & 0 \\ 0 & -q_i & p_i & 0 \\ 0 & q_i & -p_i & 0 \\ 0 & 0 & 0 & 0 \end{pmatrix}_{\mathbf{r}, \mathbf{r}+\mathbf{e}_i}. \quad (7)$$

The range of the sum $\sum_{x,y}$ depends on the boundary conditions:

$$\sum_{x,y} = \begin{cases} \sum_{x=1}^{L_x} \sum_{y=1}^{L_y} & \text{for torus boundary conditions} \\ \sum_{x=1}^{L_x-1} \sum_{y=1}^{L_y-1} & \text{for closed boundary conditions} \\ \sum_{x=1}^{L_x-1} \sum_{y=1}^{L_y} & \text{for multi-lane boundary conditions.} \end{cases} \quad (8)$$

The Markov matrix of the ASEP (6) is regarded as the non-Hermitian Hamiltonian of the quantum spin chain. When the hopping rates are symmetric ($p_i = q_i$), the Markov matrix is equivalent to the Hamiltonian of the spin-1/2 Heisenberg model.

2.2. ASEP-LK

In this paper, we focus on the 2D ASEP with Langmuir kinetics (ASEP-LK). Namely, we introduce the attachment and detachment of particles in the bulk of the ASEP in a 2D lattice with the system size $L_T = L_x \times L_y$. The updating rule is defined as follows. Particles hop to the forward site in the x -direction (y -direction) with a hopping rate p_x (p_y) and to the backward site with a hopping rate q_x (q_y). Because of the hardcore interaction, particles cannot hop to an occupied site. In the bulk, particles attach (detach) a site with a rate ω_a (ω_d). The schematic drawing of the ASEP-LK is shown in Fig. 1.

As in the case of the ASEP, the time evolution of the ASEP-LK is described by the master equation

$$\frac{d}{dt}|P(t)\rangle = \mathcal{H}_{\text{ASEP-LK}}|P(t)\rangle. \quad (9)$$

The Markov matrix is given by

$$\mathcal{H}_{\text{ASEP-LK}} = \sum_{i \in \{x,y\}} \sum_{x,y} \mathcal{M}_{\mathbf{r}, \mathbf{r} + \mathbf{e}_i} + \sum_{\mathbf{r}} h_{\mathbf{r}}, \quad (10)$$

where $h_{\mathbf{r}}$ is the term that describes the attachment and detachment of particles at the site \mathbf{r} , and it is expressed as an off-diagonal magnetic field as follows:

$$\begin{aligned} h_{\mathbf{r}} &= \omega_a \left[\hat{S}_{\mathbf{r}}^- - (1 - \hat{n}_{\mathbf{r}}) \right] + \omega_d \left[\hat{S}_{\mathbf{r}}^+ - \hat{n}_{\mathbf{r}} \right] \\ &= \begin{pmatrix} -\omega_a & \omega_d \\ \omega_a & -\omega_d \end{pmatrix}_{\mathbf{r}}. \end{aligned} \quad (11)$$

The first term of the Markov matrix (10) describes the asymmetric diffusion, and the second term describes the Langmuir kinetics. The range of the sum $\sum_{x,y}$ depends on

the boundary conditions and follows Eq. (8), and that of the sum $\sum_{\mathbf{r}}$ is all sites. In contrast to the case of the ASEP, the number of the particles N is not conserved in the ASEP-LK. For the subsequent discussion, we introduce the following constants

$$\omega := \omega_a + \omega_d, \quad \alpha := \frac{\omega_a}{\omega_d}, \quad (12)$$

which describe the strength of Langmuir kinetics and the attachment and detachment rate ratio, respectively.

3. General expression of the steady state

3.1. Steady state of the ASEP without Langmuir kinetics

In the case of the standard ASEP without Langmuir kinetics, the number of particles N is conserved. The Markov matrix (6) can be block diagonalized, and steady states exist for each subspace corresponding to the particle number N . A configuration in the N particles' subspace, which is denoted by n_N , is represented by the positions of N particles $(\mathbf{r}_1, \mathbf{r}_2, \dots, \mathbf{r}_N)$. We denote the basis of the $\binom{L_T}{N}$ -dimensional subspace as $|n_N\rangle = |(\mathbf{r}_1, \mathbf{r}_2, \dots, \mathbf{r}_N)\rangle$. A stochastic state vector with N particles in the ASEP is given by

$$|P_N(t)\rangle = \sum_{n_N} P(n_N, t) |n_N\rangle, \quad \sum_{n_N} P(n_N, t) = 1. \quad (13)$$

where $P(n_N, t)$ is the probability of the system being in n_N at time t .

When the ASEP reaches the steady states, the master equation (5) in the N particles' subspace satisfies

$$\frac{d}{dt} |P_N(t)\rangle = \mathcal{H}_{\text{ASEP}} |P_N(t)\rangle = 0. \quad (14)$$

Namely, the steady state is the eigenstate of the Markov matrix with a zero eigenvalue. We denote the steady states of the ASEP with N particles as

$$|S_N\rangle = \frac{1}{Z_N} \sum_{n_N} P_{\text{st}}(n_N) |n_N\rangle, \quad Z_N := \sum_{n_N} P_{\text{st}}(n_N). \quad (15)$$

The steady state of the multi-dimensional ASEP is constructed in Ref. [1]. In the 2D case, the steady state is given by

$$P_{\text{st}}(n_N) = \begin{cases} 1 & \text{for torus boundary conditions} \\ \left(\frac{p_x}{q_x}\right)^{\sum_{j=1}^N x_j} \left(\frac{p_y}{q_y}\right)^{\sum_{j=1}^N y_j} & \text{for closed boundary conditions} \\ \left(\frac{p_x}{q_x}\right)^{\sum_{j=1}^N x_j} & \text{for multi-lane boundary conditions,} \end{cases} \quad (16)$$

where $\mathbf{r}_j = (x_j, y_j)$ denotes the position of the j -th particle ($j = 1, 2, \dots, N$).

3.2. Steady state of the ASEP-LK

In contrast, in the case of the ASEP-LK, the number of particles N is not conserved. Therefore, unlike the standard ASEP case, we have to consider all configuration space, and there is a unique steady state. A stochastic state vector for all configuration space is expressed as

$$|P(t)\rangle = \sum_{N=0}^{L_T} \sum_{n_N} P(n_N, t) |n_N\rangle, \quad \sum_{N=0}^{L_T} \sum_{n_N} P(n_N, t) = 1. \quad (17)$$

We denote the steady state of the ASEP-LK as

$$|S_{LK}\rangle = \frac{1}{\Xi} \sum_{N=0}^{L_T} \sum_{n_N} P_{LK}(n_N) |n_N\rangle, \quad \Xi := \sum_{N=0}^{L_T} \sum_{n_N} P_{LK}(n_N). \quad (18)$$

The steady state satisfies

$$\mathcal{H}_{\text{ASEP-LK}} |S_{LK}\rangle = 0, \quad (19)$$

which indicates that $|S_{LK}\rangle$ is the zero energy eigenstate of the Markov matrix (10).

In the steady state of the ASEP-LK, the sum of the weight with fixed N satisfies the following relation, which is proved in Sec. 3.3:

$$\begin{aligned} \sum_{n_N} P_{LK}(n_N) &= \binom{L_T}{N} \alpha^N \\ &=: P_T(N). \end{aligned} \quad (20)$$

This relation indicates that the stochastic state vector of the steady state can be written in the form

$$|S_{LK}\rangle = \frac{1}{\Xi} \sum_{N=0}^{L_T} P_T(N) |P_N\rangle, \quad \Xi = (1 + \alpha)^{L_T}, \quad (21)$$

where $|P_N\rangle$ is a stochastic state vector in the subspace with N particles

$$|P_N\rangle = \sum_{n_N} P(n_N) |n_N\rangle, \quad \sum_{n_N} P(n_N) = 1. \quad (22)$$

From this, we can calculate the average density of the ASEP-LK in the steady state, which is denoted as ρ_{st} . We introduce the total number operator $\hat{N}_T := \sum_r \hat{n}_r$ and define the average density as $\rho(t) = \frac{1}{L_T} \langle \mathcal{P} | \hat{N}_T | P(t) \rangle$. From Eq. (21),

$$\begin{aligned} \rho_{\text{st}} &= \frac{1}{L_T} \langle \mathcal{P} | \hat{N}_T | S_{LK} \rangle \\ &= \frac{1}{L_T (1 + \alpha)^{L_T}} \sum_{N=0}^{L_T} N P_T(N) \\ &= \frac{\alpha}{1 + \alpha}, \end{aligned} \quad (23)$$

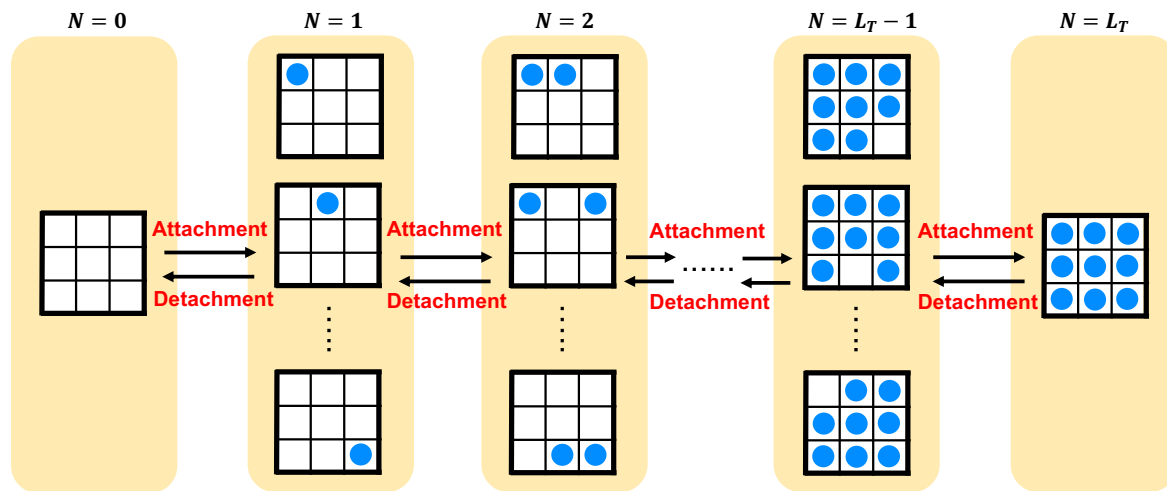


Figure 2. Transition processes of the ASEP-LK. When Langmuir kinetics rate ω is infinitesimally small, it is expected that a large number of transitions due to hopping occur between processes of the attachment and detachment of particles, achieving the steady state of the standard ASEP without Langmuir kinetics.

where we use

$$\sum_{N=0}^{L_T} N \alpha^N \binom{L_T}{N} = L_T \alpha (1 + \alpha)^{L_T - 1}. \quad (24)$$

Eq. (23) holds for all of the torus, closed, and multi-lane boundary conditions.

We call Eq. (21) general expression for the steady state of the ASEP-LK. Generally, $|P_N\rangle$ in Eq. (21) depends on the attachment and detachment rates (ω_a, ω_d). However, under the specific conditions, $|P_N\rangle$ is equal to $|S_N\rangle$, where $|S_N\rangle$ is the steady state of the standard ASEP without the Langmuir kinetics. That is,

$$|S_{LK}\rangle = \frac{1}{(1 + \alpha)^{L_T}} \sum_{N=0}^{L_T} P_T(N) |S_N\rangle \quad (25)$$

provides the steady states of the ASEP-LK. In particular, in the infinitesimal Langmuir kinetics limit ($\omega \rightarrow 0$) with the fixed attachment and detachment ratio α , the steady state is expected to be expressed as Eq. (25). In Sec. 5 and 6, we numerically confirm this conjecture under the closed and multi-lane conditions. This is interpreted as follows based on physical intuition. In the ASEP-LK, there are two types of transition processes: hopping and Langmuir kinetics (Fig. 2). When Langmuir kinetics rate ω is infinitesimally small, the frequency of transitions due to the hopping becomes significantly higher than that due to the attachment and detachment of particles. Therefore, it is expected that an enormous number of transitions due to hopping occur between processes of the attachment and detachment of particles, achieving the steady state of the standard ASEP without Langmuir kinetics. Thus, in the steady state of the ASEP-LK in infinitesimal Langmuir kinetics, $|S_N\rangle$ is realized for each particle

number sector and superposed with the weight (20). In addition, in the torus boundary conditions, we can prove that the steady state is expressed as Eq. (25) for any value of ω , as we show in Sec. 4.

3.3. Proof of the relation (20)

In the following, we prove the relation (20). We consider a configuration with N particles, which is expressed as n_N . We define a set of configurations with $N + 1$ particles, which is denoted as $A(n_N)$, by all configurations with $N + 1$ particles that can be transitioned from n_N through the attachment process. Similarly, we also define a set of configurations with $N - 1$ particles, which is denoted as $D(n_N)$, by all configurations with $N - 1$ particles that can be transitioned from n_N through the detachment process.

The master equation of the ASEP-LK (19) can be rewritten as follows:

$$\begin{aligned} \frac{dP(n_N, t)}{dt} = & \sum_{n'_N \neq n_N} [P(n'_N, t)W_h(n'_N \rightarrow n_N) - P(n_N, t)W_h(n_N \rightarrow n'_N)] \\ & + \omega_a \left[\sum_{n_{N-1} \in D(n_N)} P(n_{N-1}, t) - (L_T - N)P(n_N, t) \right] \\ & + \omega_d \left[\sum_{n_{N+1} \in A(n_N)} P(n_{N+1}, t) - NP(n_N, t) \right]. \end{aligned} \quad (26)$$

In the right-hand side of Eq. (26), the first term describes the hopping process, the second describes the attachment process, and the third describes the detachment process. When we consider the steady state, the master equation is given by

$$\begin{aligned} & \sum_{n'_N \neq n_N} [P_{\text{LK}}(n'_N)W_h(n'_N \rightarrow n_N) - P_{\text{LK}}(n_N)W_h(n_N \rightarrow n'_N)] \\ & + \omega_a \left[\sum_{n_{N-1} \in D(n_N)} P_{\text{LK}}(n_{N-1}) - (L_T - N)P_{\text{LK}}(n_N) \right] \\ & + \omega_d \left[\sum_{n_{N+1} \in A(n_N)} P_{\text{LK}}(n_{N+1}) - NP_{\text{LK}}(n_N) \right] = 0. \end{aligned} \quad (27)$$

We take the sum of the master equations Eq. (27) over all configurations with N particles. Since the sum of the first term becomes zero:

$$\sum_{n_N} \sum_{n'_N \neq n_N} [P_{\text{LK}}(n'_N)W_h(n'_N \rightarrow n_N) - P_{\text{LK}}(n_N)W_h(n_N \rightarrow n'_N)] = 0, \quad (28)$$

we obtain

$$\begin{aligned} \omega_a \sum_{n_N} \left[\sum_{n_{N-1} \in D(n_N)} P_{\text{LK}}(n_{N-1}) - (L_T - N) P_{\text{LK}}(n_N) \right] \\ + \omega_d \sum_{n_N} \left[\sum_{n_{N+1} \in A(n_N)} P_{\text{LK}}(n_{N+1}) - N P_{\text{LK}}(n_N) \right] = 0. \end{aligned} \quad (29)$$

Here, the following is satisfied

$$\begin{aligned} \sum_{n_N} \sum_{n_{N-1} \in D(n_N)} P_{\text{LK}}(n_{N-1}) &= (L_T - N + 1) \sum_{n_{N-1}} P_{\text{LK}}(n_{N-1}), \\ \sum_{n_N} \sum_{n_{N+1} \in A(n_N)} P_{\text{LK}}(n_{N+1}) &= (N + 1) \sum_{n_{N+1}} P_{\text{LK}}(n_{N+1}). \end{aligned} \quad (30)$$

For a configuration n_{N-1} (n_{N+1}), there are $L_T - N + 1$ ($N + 1$) ways to make a configuration n_N by detaching (attaching) a particle, which corresponds to the coefficient in the right-hand side of Eq. (30). Then, we obtain the difference equation for $P_t(N)$ from Eq. (29)

$$(L_T - N + 1)\alpha P_t(N - 1) - [(L_T - N)\alpha + N] P_t(N) + (N + 1)P_t(N + 1) = 0. \quad (31)$$

By substituting Eq. (20) for the left-hand side of Eq. (31), we obtain

$$\begin{aligned} \text{LHS} &= \alpha^N \left\{ (L_T - N + 1) \binom{L_T}{N - 1} \right. \\ &\quad \left. - [(L_T - N)\alpha + N] \binom{L_T}{N} + (N + 1)\alpha \binom{L_T}{N + 1} \right\} \\ &= 0. \end{aligned} \quad (32)$$

Namely, Eq. (20) is a solution of the difference equation (31). Therefore, in the steady state of the ASEP-LK, the relation (20) is satisfied.

4. Steady state in the torus boundary conditions

In this section, we construct the exact steady state of the ASEP-LK in the torus boundary conditions and show that it corresponds to Eq. (25). When considering the periodic boundary conditions, even if the hopping rates are extended inhomogeneous for each lane ($p_x \rightarrow p_x(y)$, $p_y \rightarrow p_y(x)$), we can still discuss the construction of the steady state similarly. Therefore, we consider the Markov matrix extended as follows:

$$\mathcal{H}_{\text{ASEP-LK}} = \sum_{x=1}^{L_x} \sum_{y=1}^{L_y} [\mathcal{M}_{\mathbf{r}, \mathbf{r} + \mathbf{e}_x}(y) + \mathcal{M}_{\mathbf{r}, \mathbf{r} + \mathbf{e}_y}(x)] + \sum_{\mathbf{r}} h_{\mathbf{r}}, \quad (33)$$

where

$$\mathcal{M}_{\mathbf{r}, \mathbf{r} + \mathbf{e}_i}(j) = \begin{pmatrix} 0 & 0 & 0 & 0 \\ 0 & -q_i(j) & p_i(j) & 0 \\ 0 & q_i(j) & -p_i(j) & 0 \\ 0 & 0 & 0 & 0 \end{pmatrix}_{\mathbf{r}, \mathbf{r} + \mathbf{e}_i}. \quad (34)$$

Here, we define the $2^{L_t} \times 2^{L_t}$ matrix U , which is originally introduced in the 1D case [46], as

$$U = \underbrace{\begin{pmatrix} 1 & 1 \\ \alpha & -1 \end{pmatrix} \otimes \begin{pmatrix} 1 & 1 \\ \alpha & -1 \end{pmatrix} \otimes \cdots \otimes \begin{pmatrix} 1 & 1 \\ \alpha & -1 \end{pmatrix}}_{L_T}, \quad (35)$$

and transform the Markov matrix (33) as follows:

$$\begin{aligned} \tilde{\mathcal{H}}_{\text{ASEP-LK}} &= U^{-1} \mathcal{H}_{\text{ASEP-LK}} U \\ &= \sum_{x=1}^{L_x} \sum_{y=1}^{L_y} \left[\tilde{\mathcal{M}}_{\mathbf{r}, \mathbf{r} + \mathbf{e}_x}(y) + \tilde{\mathcal{M}}_{\mathbf{r}, \mathbf{r} + \mathbf{e}_y}(x) \right] + \sum_{\mathbf{r}} \tilde{h}_{\mathbf{r}}. \end{aligned} \quad (36)$$

$\tilde{\mathcal{M}}_{\mathbf{r}, \mathbf{r} + \mathbf{e}_i}(j)$ and $\tilde{h}_{\mathbf{r}}$ are given by

$$\tilde{\mathcal{M}}_{\mathbf{r}, \mathbf{r} + \mathbf{e}_i}(j) = \frac{1}{1 + \alpha} \begin{pmatrix} 0 & 0 & 0 & 0 \\ -a(j) & -b(j) & c(j) & d(j) \\ a(j) & b(j) & -c(j) & -d(j) \\ 0 & 0 & 0 & 0 \end{pmatrix}_{\mathbf{r}, \mathbf{r} + \mathbf{e}_i} \quad (37)$$

$$\tilde{h}_{\mathbf{r}} = -\omega \begin{pmatrix} 0 & 0 \\ 0 & 1 \end{pmatrix}_{\mathbf{r}}, \quad (38)$$

where

$$\begin{aligned} a(j) &= \alpha(p_i(j) - q_i(j)), \\ b(j) &= q_i(j) + p_i(j)\alpha, \\ c(j) &= p_i(j) + q_i(j)\alpha, \\ d(j) &= p_i(j) - q_i(j). \end{aligned} \quad (39)$$

We introduce the reference state $|\text{vac}\rangle$ defined as

$$|\text{vac}\rangle := \underbrace{|0\rangle \otimes |0\rangle \otimes \cdots \otimes |0\rangle}_{L_T}, \quad (40)$$

where we denote an empty state as $|0\rangle := (1, 0)^T$ and an occupied state as $|1\rangle := (0, 1)^T$. The reference state is a zero energy eigenstate of the transformed Markov matrix (36):

$$\tilde{\mathcal{H}}_{\text{ASEP-LK}} |\text{vac}\rangle = 0. \quad (41)$$

This is confirmed as follows. From Eq. (37) and (38),

$$\tilde{\mathcal{M}}_{\mathbf{r},\mathbf{r}+\mathbf{e}_i}(j)|\text{vac}\rangle = \frac{a(j)}{1+\alpha}(|\mathbf{r}\rangle - |\mathbf{r} + \mathbf{e}_i\rangle) \quad (42)$$

$$\tilde{h}_{\mathbf{r}}|\text{vac}\rangle = 0, \quad (43)$$

where $|\mathbf{r}\rangle$ indicates the configuration where a single particle exist at site \mathbf{r} . Then,

$$\begin{aligned} \tilde{\mathcal{H}}_{\text{ASEP-LK}}|\text{vac}\rangle &= \left\{ \sum_{x=1}^{L_x} \sum_{y=1}^{L_y} \left[\tilde{\mathcal{M}}_{\mathbf{r},\mathbf{r}+\mathbf{e}_x}(y) + \tilde{\mathcal{M}}_{\mathbf{r},\mathbf{r}+\mathbf{e}_y}(x) \right] + \sum_{\mathbf{r}} \tilde{h}_{\mathbf{r}} \right\} |\text{vac}\rangle \\ &= \sum_{y=1}^{L_y} \frac{a(y)}{1+\alpha} \sum_{x=1}^{L_x} (|\mathbf{r}\rangle - |\mathbf{r} + \mathbf{e}_x\rangle) + \sum_{x=1}^{L_x} \frac{a(x)}{1+\alpha} \sum_{y=1}^{L_y} (|\mathbf{r}\rangle - |\mathbf{r} + \mathbf{e}_y\rangle) \\ &= 0. \end{aligned} \quad (44)$$

By considering the inverse transformation of $|\text{vac}\rangle$, we can construct the zero energy eigenstate of the Markov matrix $\mathcal{H}_{\text{ASEP-LK}}$:

$$\begin{aligned} |\bar{S}_{\text{LK}}\rangle &= U|\text{vac}\rangle \\ &= \underbrace{\begin{pmatrix} 1 \\ \alpha \end{pmatrix} \otimes \begin{pmatrix} 1 \\ \alpha \end{pmatrix} \otimes \cdots \otimes \begin{pmatrix} 1 \\ \alpha \end{pmatrix}}_{L_{\text{T}}} \\ &= \sum_{N=0}^{L_{\text{T}}} \alpha^N \sum_{n_N} |n_N\rangle \\ &= \sum_{N=0}^{L_{\text{T}}} \binom{L_{\text{T}}}{N} \alpha^N |S_N\rangle. \end{aligned} \quad (45)$$

Although $|\bar{S}_{\text{LK}}\rangle$ is the eigenstates:

$$\mathcal{H}_{\text{ASEP-LK}}|\bar{S}_{\text{LK}}\rangle = U\tilde{\mathcal{H}}_{\text{ASEP-LK}}|\text{vac}\rangle = 0, \quad (46)$$

$|\bar{S}_{\text{LK}}\rangle$ is not a stochastic state vector and needs to be normalized. Since $\sum_{N=0}^{L_{\text{T}}} \binom{L_{\text{T}}}{N} \alpha^N = (1+\alpha)^{L_{\text{T}}}$, the steady state is given by

$$|S_{\text{LK}}\rangle = \frac{1}{(1+\alpha)^{L_{\text{T}}}} \sum_{N=0}^{L_{\text{T}}} \binom{L_{\text{T}}}{N} \alpha^N |S_N\rangle. \quad (47)$$

This expression is identical to the proposed steady state (25).

In the following, we evaluate the physical quantities in the steady state. We introduce the local density $\rho(\mathbf{r})$ as

$$\rho(\mathbf{r}) := \langle \mathcal{P} | \hat{n}_{\mathbf{r}} | P(t) \rangle, \quad (48)$$

and the quasi-one-dimensional current $j_{x,\bar{x}}(j_{y,\bar{y}})$, which represents the current in the x -direction (y -direction) at the cross-section $x = \bar{x}$ ($y = \bar{y}$), as

$$j_{x,\bar{x}} := \langle \mathcal{P} | \hat{j}_{x,\bar{x}} | P(t) \rangle, \quad j_{y,\bar{y}} := \langle \mathcal{P} | \hat{j}_{y,\bar{y}} | P(t) \rangle, \quad (49)$$

where we introduce the quasi-one-dimensional current operator $\hat{j}_{x,\bar{x}}(\hat{j}_{y,\bar{y}})$ as follows:

$$\begin{aligned} \hat{j}_{x,\bar{x}} &:= \sum_{y=1}^{L_y} [p_x(y) \hat{n}_{(\bar{x},y)} (1 - \hat{n}_{(\bar{x}+1,y)}) - q_x(y) (1 - \hat{n}_{(\bar{x},y)}) \hat{n}_{(\bar{x}+1,y)}], \\ \hat{j}_{y,\bar{y}} &:= \sum_{x=1}^{L_x} [p_y(x) \hat{n}_{(x,\bar{y})} (1 - \hat{n}_{(x,\bar{y}+1)}) - q_y(x) (1 - \hat{n}_{(x,\bar{y})}) \hat{n}_{(x,\bar{y}+1)}]. \end{aligned} \quad (50)$$

In the case of the ASEP without Langmuir kinetics, the local density $\rho_N(\mathbf{r})$ and the quasi-one-dimensional current $j_{N;x,\bar{x}}(j_{N;y,\bar{y}})$ in the steady state (15) is given by

$$\rho_N(\mathbf{r}) = \langle \mathcal{P} | \hat{n}_{\mathbf{r}} | S_N \rangle = \frac{N}{L_T}, \quad (51)$$

$$j_{N;i,\bar{i}} = \langle \mathcal{P} | \hat{j}_{i,\bar{i}} | S_N \rangle = \sum_{k=1}^{L_k} [p_i(k) - q_i(k)] \frac{N(L_T - N)}{L_T(L_T - 1)}, \quad (i, k = x, y, \quad k \neq i). \quad (52)$$

Then, we calculate the local density for the ASEP-LK from Eq. (47), Eq. (48), and Eq. (51) as follows:

$$\begin{aligned} \rho_{\text{st}}(\mathbf{r}) &= \langle \mathcal{P} | \hat{n}_{\mathbf{r}} | S_{\text{LK}} \rangle \\ &= \frac{1}{(1 + \alpha)^{L_T}} \sum_{N=0}^{L_T} \binom{L_T}{N} \alpha^N \rho_N(\mathbf{r}) \\ &= \frac{\alpha}{1 + \alpha}. \end{aligned} \quad (53)$$

This is equal to the average density (23) since the stationary distribution of particles is spatially uniform in the torus boundary conditions case. Similarly, the quasi-one-dimensional current $j_{x,\bar{x}}(j_{y,\bar{y}})$ in the steady state of the ASEP-LK is obtained from Eq. (47), Eq. (48), and Eq. (52) as follows:

$$\begin{aligned} j_{i,\bar{i}} &:= \langle \mathcal{P} | \hat{j}_{i,\bar{i}} | S_{\text{LK}} \rangle \\ &= \frac{1}{(1 + \alpha)^{L_T}} \sum_{N=0}^{L_T} \binom{L_T}{N} \alpha^N \hat{j}_{N;i,\bar{i}}(\mathbf{r}) \\ &= \sum_{k=1}^{L_k} [p_i(k) - q_i(k)] \frac{\alpha}{1 + \alpha} \left(1 - \frac{\alpha}{1 + \alpha} \right) \\ &= \sum_{k=1}^{L_k} [p_i(k) - q_i(k)] \rho_{\text{st}} (1 - \rho_{\text{st}}) \quad (i, k = x, y, \quad k \neq i). \end{aligned} \quad (54)$$

In the standard ASEP without Langmuir kinetics, the quasi-one-dimensional current (52) depends on the system size L_T . In contrast, in the case of the ASEP-LK, the quasi-one-dimensional current (54) does not depend on the system size L_T . This result is consistent with the 1D case [45, 46].

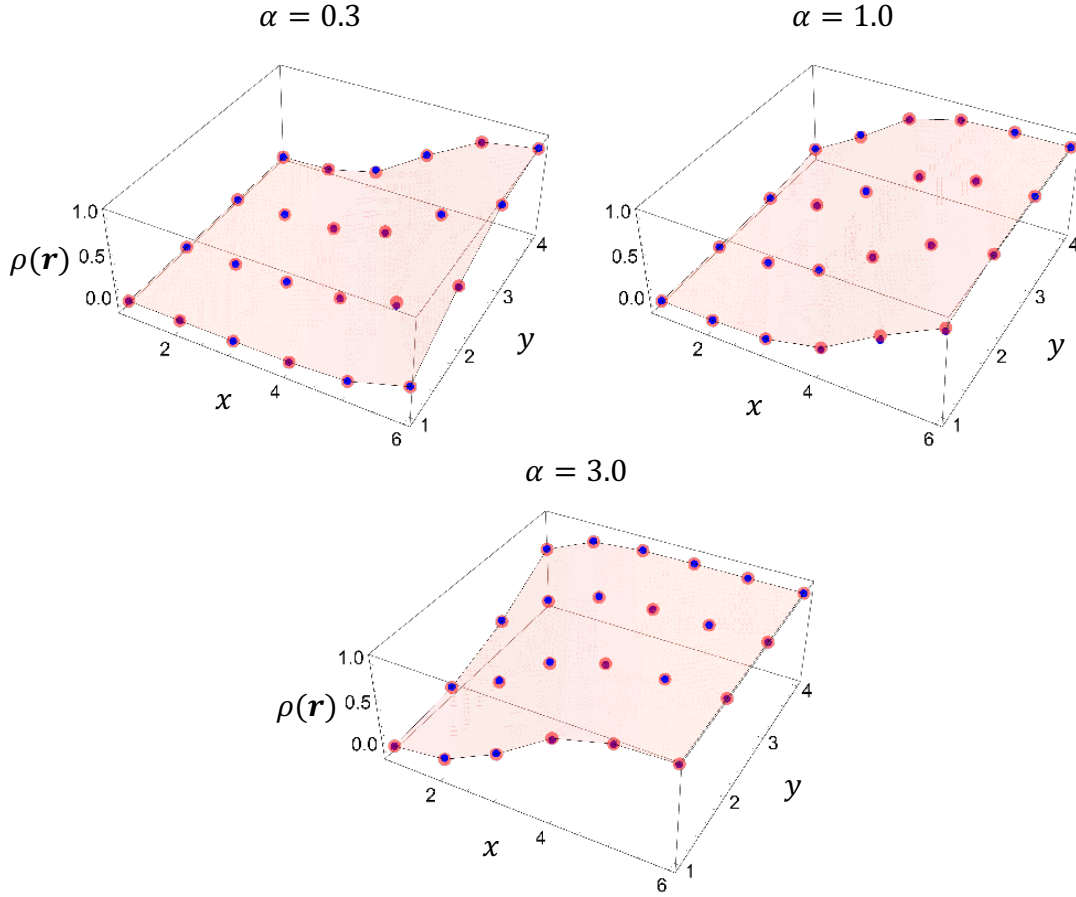


Figure 3. Local density of the ASEP-LK in the closed boundary conditions for various α . We set the parameters as $(p_x, q_x, p_y, q_y) = (1.0, 0.1, 0.8, 0.1)$ and $(L_x, L_y) = (6, 4)$. Red dots represent the results from Eq. (58), and blue dots represent those from Monte Carlo simulations.

5. Steady state in the closed boundary conditions

In this section, we consider the closed boundary conditions where the Markov matrix is given by

$$\mathcal{H}_{\text{ASEP-LK}} = \sum_{x=1}^{L_x-1} \sum_{y=1}^{L_y-1} [\mathcal{M}_{\mathbf{r}, \mathbf{r}+\mathbf{e}_x} + \mathcal{M}_{\mathbf{r}, \mathbf{r}+\mathbf{e}_y}] + \sum_{\mathbf{r}} h_{\mathbf{r}}. \quad (55)$$

Unlike the torus boundary conditions, $|P_N\rangle$ in the general expression for the steady state (21) depends on ω_a and ω_d . However, in the case of the infinitesimal Langmuir kinetics ($\omega \rightarrow 0$) with the fixed ratio of the attachment and detachment rates α , Eq. (25) is expected to be the steady state. We numerically confirmed that

$$|S_{LK}\rangle = \frac{1}{(1+\alpha)^{L_T}} \sum_{N=0}^{L_T} \sum_{n_N} P_T(N) \left(\frac{p_x}{q_x}\right)^{\sum_{j=1}^N x_j} \left(\frac{p_y}{q_y}\right)^{\sum_{j=1}^N y_j} |n_N\rangle \quad (56)$$

gives the steady state of the ASEP-LK with the closed boundary conditions.

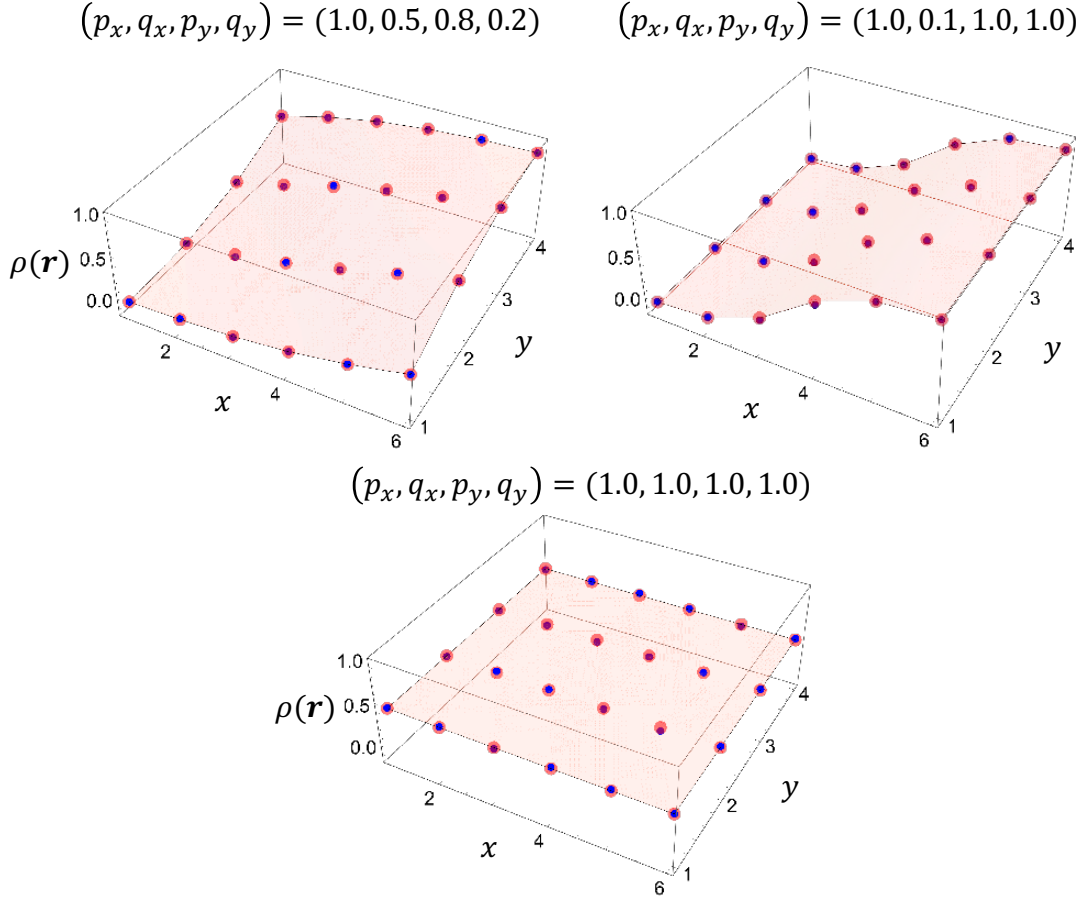


Figure 4. Local density of the ASEP-LK in the closed boundary conditions for various hopping rates (p_x, q_x, p_y, q_y) . We set the parameters as $\alpha = 1.0$ and $(L_x, L_y) = (6, 4)$. Red dots represent the results from Eq. (58), and blue dots represent those from Monte Carlo simulations.

In the standard ASEP without Langmuir kinetics, the local density $\rho_N(\mathbf{r})$ of the steady state is given by

$$\begin{aligned} \rho_N(\mathbf{r}) &= \langle \mathcal{P} | \hat{n}_{\mathbf{r}} | S_N \rangle \\ &= \frac{1}{Z_N} \sum_{\tilde{n}_N} \left(\frac{p_x}{q_x} \right)^{\sum_{j=1}^N x_j} \left(\frac{p_y}{q_y} \right)^{\sum_{j=1}^N y_j}, \end{aligned} \quad (57)$$

where $\sum_{\tilde{n}_N}$ represents the sum over all configurations with $n_{\mathbf{r}} = 1$ in the subspace of N particles. Then, the local density of the steady state in the ASEP-LK is expressed as follows:

$$\begin{aligned} \rho_{\text{st}}(\mathbf{r}) &= \langle \mathcal{P} | \hat{n}_{\mathbf{r}} | S_{\text{LK}} \rangle \\ &= \frac{1}{(1 + \alpha)^{L_T}} \sum_{N=0}^{L_T} \binom{L_T}{N} \alpha^N \rho_N(\mathbf{r}). \end{aligned} \quad (58)$$

Fig.3 and Fig. 4 show the local density of the steady state in the ASEP-LK, which are computed from both the exact expression (58) and Monte Carlo simulations. Red

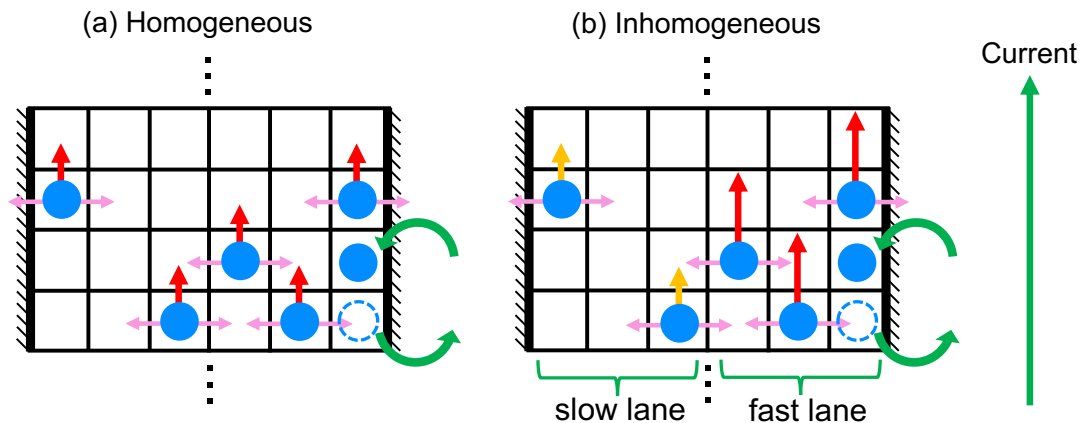


Figure 5. Examples of (a) Homogeneous and (b) inhomogeneous multi-lane ASEP with Langmuir kinetics. The hopping rate in the y -direction can be extended to be inhomogeneous for each lane in the multi-lane boundary conditions.

dots represent the results from Eq. (58), and blue dots represent those from Monte Carlo simulations. These figures indicate that the results obtained from Eq. (58) are consistent with those computed from Monte Carlo simulations. These results strongly suggest that Eq. (56) gives the exact stationary state of the ASEP-LK.

In the following, we discuss the properties of the steady state with respect to the attachment and detachment ratio α and hopping rates (p_x, q_x, p_y, q_y) . Fig. 3 shows the local density for various attachment and detachment ratios α . The size of the high-density and the low-density areas change depending on the value α . As α increases (decreases), the size of the high-density area becomes large (small). Fig. 4 shows the local density for various hopping rates (p_x, q_x, p_y, q_y) . The magnitude of the gradient between the high-density and low-density areas changes depending on the value of the hopping rates. As the asymmetry of the hopping rates increases, the gradient becomes steeper.

6. Steady state in the multi-lane boundary conditions

In this section, we discuss the steady state in the multi-lane boundary conditions, considering the closed boundary conditions in the x -direction and the periodic boundary conditions in the y -direction. In the case of the multi-lane boundary condition, the steady state can be constructed even if the hopping rate in the y -direction is extended to be inhomogeneous for each lane ($p_y \rightarrow p_y(x)$) as shown in Fig. 5. The Markov matrix of the ASEP-LK in the multi-lane boundary conditions is given by

$$\mathcal{H}_{\text{ASEP-LK}} = \sum_{x=1}^{L_x-1} \sum_{y=1}^{L_y} [\mathcal{M}_{\mathbf{r}, \mathbf{r}+\mathbf{e}_x} + \mathcal{M}_{\mathbf{r}, \mathbf{r}+\mathbf{e}_y}(x)] + \sum_{\mathbf{r}} h_{\mathbf{r}}. \quad (59)$$

As in the case of the closed boundary conditions, Eq. (25) is expected to give the steady state of the ASEP-LK (59) in the infinitesimal Langmuir kinetics $\omega \rightarrow 0$ with the fixed

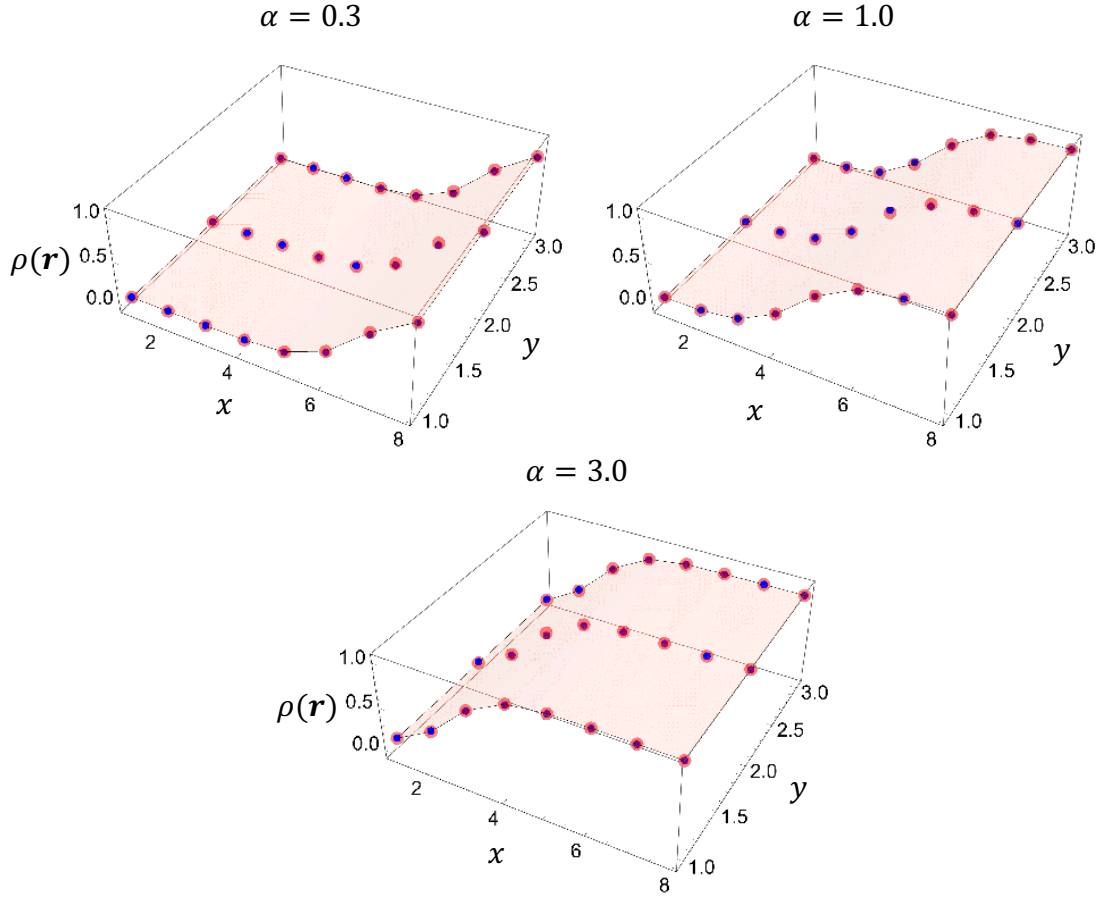


Figure 6. Local density of the ASEP-LK in the multi-lane boundary conditions for various α . We set the parameters as $(p_x, q_x) = (1.0, 0.1)$ and $(L_x, L_y) = (8, 3)$. Red dots represent the results from Eq. (63), and blue dots represent those from Monte Carlo simulations.

attachment and detachment ratio α . We numerically confirmed that

$$|S_{LK}\rangle = \frac{1}{(1 + \alpha)^{L_T}} \sum_{N=0}^{L_T} \sum_{n_N} P_T(N) \left(\frac{p_x}{q_x} \right)^{\sum_{j=1}^N x_j} |n_N\rangle \quad (60)$$

is the steady state of the ASEP-LK in the multi-lane boundary conditions.

In the standard ASEP without Langmuir kinetics, the local density $\rho_N(\mathbf{r})$ of the steady state (15) is given by

$$\begin{aligned} \rho_N(\mathbf{r}) &= \langle \mathcal{P} | \hat{n}_{\mathbf{r}} | S_N \rangle \\ &= \frac{1}{Z_N} \sum_{\tilde{n}_N} \left(\frac{p_x}{q_x} \right)^{\sum_{j=1}^N x_j}, \end{aligned} \quad (61)$$

where $\sum_{\tilde{n}_N}$ represents the sum over all configurations with $n_{\mathbf{r}} = 1$ in the subspace of N

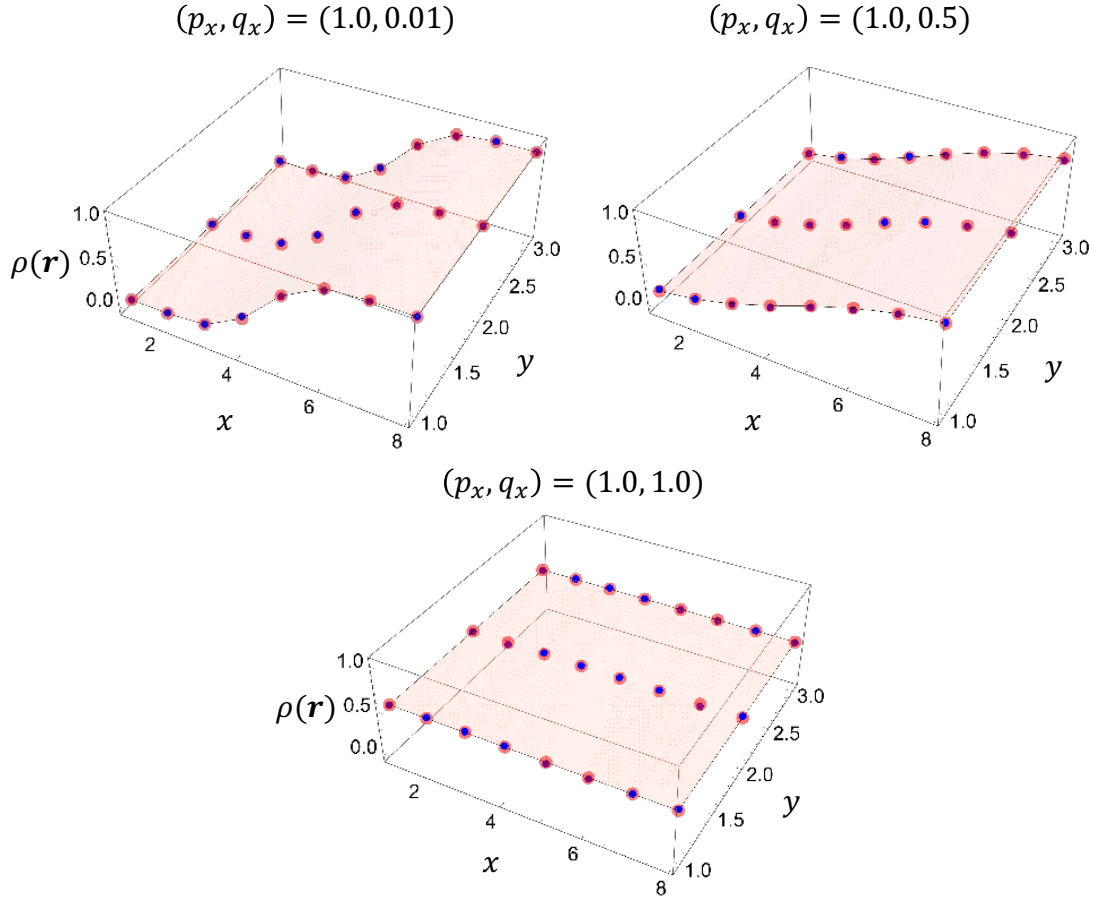


Figure 7. Local density of the ASEP-LK in the multi-lane boundary conditions for various hopping rates (p_x, q_x) . We set the parameters as $\alpha = 1.0$ and $(L_x, L_y) = (8, 3)$. Red dots represent the results from Eq. (63), and blue dots represent those from Monte Carlo simulations.

particles. Similarly, the quasi-one-dimensional current $j_{N;y,\bar{y}}$ of the steady state (15) is

$$\begin{aligned}
 j_{N;y,\bar{y}} &= \langle \mathcal{P} | \hat{j}_{y,\bar{y}} | S_N \rangle \\
 &= \frac{1}{Z_N} \sum_{x=1}^{L_x} \left[\sum_{\bar{n}_{N;f}} p_y(x) \left(\frac{p_x}{q_x} \right)^{\sum_{j=1}^N x_j} - \sum_{\bar{n}_{N;b}} q_y(x) \left(\frac{p_x}{q_x} \right)^{\sum_{j=1}^N x_j} \right], \quad (62)
 \end{aligned}$$

where $\sum_{\bar{n}_{N;f}}$ ($\sum_{\bar{n}_{N;b}}$) represents the sum over all configurations with $n_{\mathbf{r}} = 1$ and $n_{\mathbf{r}+\mathbf{e}_y} = 0$ ($n_{\mathbf{r}} = 0$ and $n_{\mathbf{r}+\mathbf{e}_y} = 1$) in the subspace of N particles. Then, the local density $\rho_{\text{st}}(\mathbf{r})$ and the quasi-one-dimensional current in the y -direction $j_{y,\bar{y}}$ of the steady

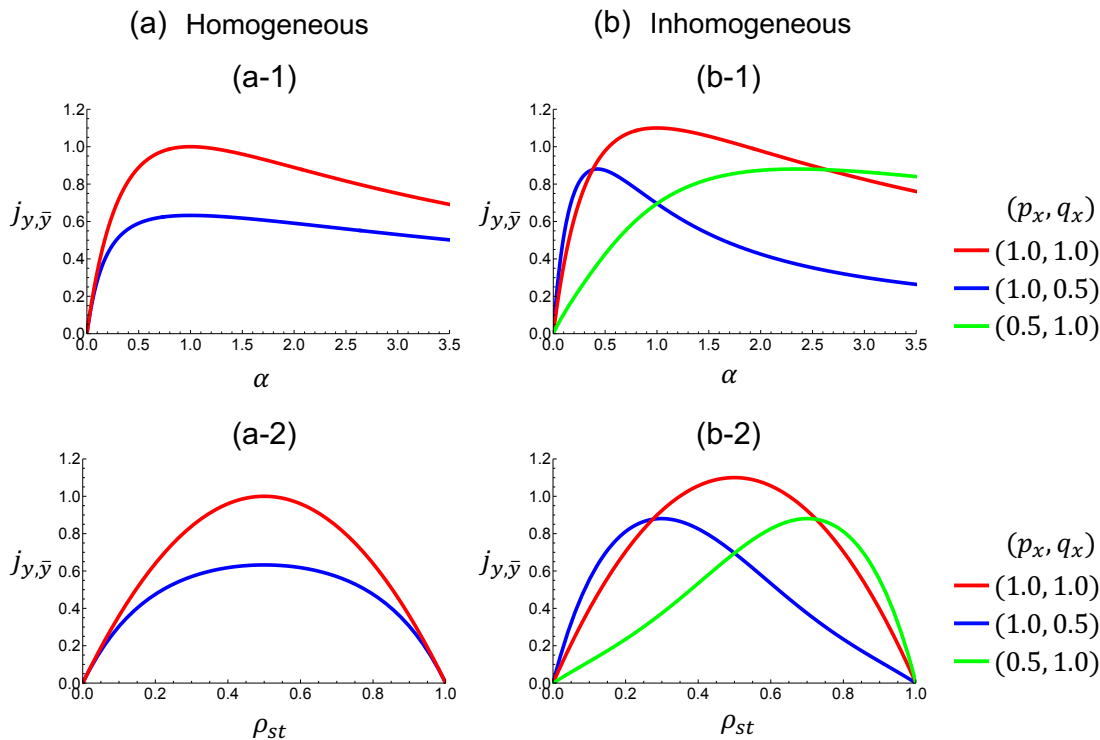


Figure 8. Quasi-one-dimensional current $j_{y,\bar{y}}$ with respect to the attachment and detachment ratio α and the average density ρ_{st} . We set the parameters as $(L_x, L_y) = (8, 3)$, $q_y = 0$, and $\bar{y} = 1$. (a) Homogeneous hopping rate in y -direction ($p_y(x) = 0.5$). (b) Inhomogeneous hopping rate in y direction ($p_y(x) = 0.1$ for $1 \leq x \leq L_x/2$, and $p_y(x) = 1.0$ for $L_x/2 < x \leq L_x$).

state in the ASEP-LK (60) is expressed as follows:

$$\begin{aligned} \rho_{st}(\mathbf{r}) &= \langle \mathcal{P} | \hat{n}_{\mathbf{r}} | S_{LK} \rangle \\ &= \frac{1}{(1 + \alpha)^{L_T}} \sum_{N=0}^{L_T} \binom{L_T}{N} \alpha^N \rho_N(\mathbf{r}), \end{aligned} \quad (63)$$

$$\begin{aligned} j_{y,\bar{y}} &= \langle \mathcal{P} | \hat{j}_{y,\bar{y}} | S_{LK} \rangle \\ &= \frac{1}{(1 + \alpha)^{L_T}} \sum_{N=0}^{L_T} \binom{L_T}{N} \alpha^N j_{N;y,\bar{y}}. \end{aligned} \quad (64)$$

Fig. 6 and Fig. 7 show the local density of the steady state in the multi-lane boundary conditions, which are obtained from both the exact expression (63) and Monte Carlo simulations. Red dots represent the results from Eq. (63), and blue dots represent those from Monte Carlo simulations. These figures indicate that the results obtained from Eq. (63) are consistent with those computed from Monte Carlo simulations. These results strongly suggest that Eq. (60) is the exact stationary state of the ASEP-LK in the multi-lane boundary conditions.

Fig. 6 shows the local density for various attachment and detachment ratio α , and Fig. 7 shows that for various hopping rates (p_x, q_x) . As in the case of the closed

boundary conditions, the size of the high- and low-density areas depends on the value α , and the magnitude of the gradient between high- and low-density areas depends on the asymmetry of the hopping rates (p_x, q_x) .

Fig. 8 shows the quasi-one-dimensional current $j_{y,\bar{y}}$ in the steady state, which is calculated from Eq. (64). Figs. 8 (a) show the results of the homogeneous multi-lane ASEP-LK where the hopping rates are uniform ($p_y(x) = 0.5$), and Figs. 8 (b) shows those of the inhomogeneous multi-lane ASEP-LK where the hopping rates are non-uniform for each lane ($p_y(x) = 0.1$ for $1 \leq x \leq L_x/2$, and $p_y(x) = 0.1$ for $L_x/2 < x \leq 1$). From the results, we find that the quasi-one-dimensional current depends on the hopping rates perpendicular to the current direction. The behavior differs depending on whether the hopping rate along the current direction is homogeneous or inhomogeneous across the lanes. Figs. 8 (a-1) and (a-2) show that, in the case of the hopping rates are homogeneous, the quasi-one-dimensional current is larger when the hopping rates in the x -direction are symmetric ($p_x = q_x$) compared to when they are asymmetric ($p_x \neq q_x$). In contrast, in the hopping rates $p_y(x)$ are inhomogeneous (Figs. 8 (b-1) and (b-2)), there are regions where the current takes on larger value when the hopping rates are asymmetric than when they are symmetric.

7. Conclusion

In this paper, we considered the 2D ASEP-LK, where particle number conservation is violated. We obtained the general expression for the steady state of the ASEP-LK, which indicates that the steady state is constructed from the superposition of the steady states of the ASEP without Langmuir kinetics. By applying the result of the 2D ASEP in Ref. [1], we obtained the exact steady state of the ASEP-LK under the periodic boundary conditions and that in infinitesimal Langmuir kinetics under the closed and multi-lane boundary conditions. Based on the analytical expression, we evaluated the density and the quasi-one-dimensional current in the steady state. In the closed and multi-lane boundary conditions, the density distribution is non-uniform. High- and low-density areas co-exist, and the size depends on the attachment and detachment ratio α . In addition, we clarified the effect of two-dimensionality on the quasi-one-dimensional current. The quasi-one-dimensional current in the multi-lane boundary conditions depends on the hopping rates perpendicular to the current direction. When the hopping rates along the current are uniform among lines, the asymmetry of the perpendicular hopping rates reduces the current. However, when the hopping rates along the current are inhomogeneous among lanes, the asymmetry of the perpendicular hopping rates can become larger, depending on the value of α .

Acknowledgement

The authors thank Masataka Watanabe for fruitful discussions. This work was supported by JSPS KAKENHI Grant Number JP24K16976.

References

- [1] Ishiguro Y and Sato J 2024 Exact steady states in the asymmetric simple exclusion process beyond one dimension *arXiv preprint arXiv:2403.01934*
- [2] MacDonald C T, Gibbs J H and Pipkin A C 1968 Kinetics of biopolymerization on nucleic acid templates *Biopolymers* **6** 1–25
- [3] Klumpp S and Lipowsky R 2003 Traffic of molecular motors through tube-like compartments *J. Stat. Phys.* **113** 233–268
- [4] Schadschneider A 2000 Statistical physics of traffic flow *Physica A* **285** 101–120
- [5] Schadschneider A, Chowdhury D and Nishinari K 2010 *Stochastic transport in complex systems: from molecules to vehicles* (Elsevier)
- [6] Derrida B, Evans M R, Hakim V and Pasquier V 1993 Exact solution of a 1d asymmetric exclusion model using a matrix formulation *J. Phys. A: Math. Theor.* **26** 1493
- [7] Derrida B 1998 An exactly soluble non-equilibrium system: the asymmetric simple exclusion process *Phys. Rep.* **301** 65–83
- [8] Blythe R A and Evans M R 2007 Nonequilibrium steady states of matrix-product form: a solver’s guide *J. Phys. A: Math. Theor.* **40** R333
- [9] Crampe N, Ragoucy E and Vanicat M 2014 Integrable approach to simple exclusion processes with boundaries. review and progress *J. Phys. Mech.: Theory Exp.* P11032
- [10] Essler F H and Rittenberg V 1996 Representations of the quadratic algebra and partially asymmetric diffusion with open boundaries *J. Phys. A: Math. Gen.* **29** 3375
- [11] Golinelli O and Mallick K 2006 The asymmetric simple exclusion process: an integrable model for non-equilibrium statistical mechanics *J. Phys. A: Math. Gen.* **39** 12679
- [12] Gwa L H and Spohn H 1992 Bethe solution for the dynamical-scaling exponent of the noisy Burgers equation *Phys. Rev. A* **46** 844
- [13] Kim D 1995 Bethe ansatz solution for crossover scaling functions of the asymmetric XXZ chain and the Kardar-Parisi-Zhang-type growth model *Phys. Rev. E* **52** 3512
- [14] Golinelli O and Mallick K 2004 Bethe ansatz calculation of the spectral gap of the asymmetric exclusion process *J. Phys. A: Math. Gen.* **37** 3321
- [15] Golinelli O and Mallick K 2005 Spectral gap of the totally asymmetric exclusion process at arbitrary filling *J. Phys. A: Math. Gen.* **38** 1419
- [16] Motegi K, Sakai K and Sato J 2012 Exact relaxation dynamics in the totally asymmetric simple exclusion process *Phys. Rev. E* **85**(4) 042105
- [17] Motegi K, Sakai K and Sato J 2012 Long time asymptotics of the totally asymmetric simple exclusion process *J. Phys. A: Math. Theor.* **45** 465004
- [18] Prolhac S 2013 Spectrum of the totally asymmetric simple exclusion process on a periodic lattice—bulk eigenvalues *J. Phys. A: Math. Theor.* **46** 415001
- [19] Prolhac S 2014 Spectrum of the totally asymmetric simple exclusion process on a periodic lattice—first excited states *J. Phys. A: Math. Theor.* **47** 375001
- [20] Prolhac S 2016 Extrapolation methods and Bethe ansatz for the asymmetric exclusion process *J. Phys. A: Math. Theor.* **49** 454002
- [21] Prolhac S 2017 Perturbative solution for the spectral gap of the weakly asymmetric exclusion process *J. Phys. A: Math. Theor.* **50** 315001
- [22] Ishiguro Y, Sato J and Nishinari K 2023 Asymmetry-induced delocalization transition in the integrable non-hermitian spin chain *Phys. Rev. Res.* **5**(3) 033102
- [23] De Gier J and Essler F H 2005 Bethe ansatz solution of the asymmetric exclusion process with open boundaries *Phys. Rev. Lett.* **95** 240601
- [24] de Gier J and Essler F H L 2006 Exact spectral gaps of the asymmetric exclusion process with open boundaries *J. Stat. Mech.: Theory Exp.* **2006** P12011
- [25] de Gier J and Essler F H L 2008 Slowest relaxation mode of the partially asymmetric exclusion process with open boundaries *J. Phys. A: Math. Theor.* **41** 485002

- [26] de Gier J and Essler F H L 2011 Large Deviation Function for the Current in the Open Asymmetric Simple Exclusion Process *Phys. Rev. Lett.* **107**(1) 010602
- [27] Wen F K, Yang Z Y, Cui S, Cao J P and Yang W L 2015 Spectrum of the Open Asymmetric Simple Exclusion Process with Arbitrary Boundary Parameters *Chin. Phys. Lett.* **32** 050503
- [28] Crampé N 2015 Algebraic Bethe ansatz for the totally asymmetric simple exclusion process with boundaries *J. Phys. A: Math. Theor.* **48** 08FT01
- [29] Sandow S and Schütz G 1994 On $uq[\text{su}(2)]$ -symmetric driven diffusion *Europhys. Lett.* **26** 7
- [30] Schütz G M 1997 Duality relations for asymmetric exclusion processes *J. Stat. Phys.* **86** 1265–1287
- [31] Ishiguro Y, Sato J and Nishinari K 2021 Relationships among the asymmetric simple exclusion process, the burgers equation and the derivative nonlinear schrödinger equation *J. Phys. Soc. Jpn.* **90** 114008
- [32] Bertini L and Giacomin G 1997 Stochastic Burgers and KPZ equations from particle systems *Commun. Math. Phys.* **183** 571–607
- [33] Sasamoto T and Spohn H 2010 One-dimensional kardar-parisi-zhang equation: An exact solution and its universality *Phys. Rev. Lett.* **104**(23) 230602
- [34] Pronina E and Kolomeisky A B 2004 Two-channel totally asymmetric simple exclusion processes *J. Phys. A: Math. Theor.* **37** 9907
- [35] Tsekouras K and Kolomeisky A B 2008 Parallel coupling of symmetric and asymmetric exclusion processes *J. Phys. A: Math. Theor.* **41** 465001
- [36] Ezaki T and Nishinari K 2011 Exact solution of a heterogeneous multilane asymmetric simple exclusion process *Phys. Rev. E* **84**(6) 061141
- [37] Ezaki T and Nishinari K 2012 A balance network for the asymmetric simple exclusion process *J. Phys. Mech.: Theory Exp.* **2012** P11002
- [38] Lee H W, Popkov V and Kim D 1997 Two-way traffic flow: Exactly solvable model of traffic jam *J. Phys. A: Math. Theor.* **30** 8497
- [39] Fouladvand M E and Lee H W 1999 Exactly solvable two-way traffic model with ordered sequential update *Phys. Rev. E* **60**(6) 6465–6479
- [40] Wang Y Q, Jia B, Jiang R, Gao Z Y, Li W H, Bao K J and Zheng X Z 2017 Dynamics in multi-lane taseps coupled with asymmetric lane-changing rates *Nonlinear Dyn.* **88** 2051–2061
- [41] Wang Y Q, Wang J X, Li W H, Zhou C F and Jia B 2018 Analytical and simulation studies of driven diffusive system with asymmetric heterogeneous interactions *Sci. Rep.* **8** 16287
- [42] Parmeggiani A, Franosch T and Frey E 2003 Phase coexistence in driven one-dimensional transport *Phys. Rev. Lett.* **90**(8) 086601
- [43] Parmeggiani A, Franosch T and Frey E 2004 Totally asymmetric simple exclusion process with langmuir kinetics *Phys. Rev. E* **70**(4) 046101
- [44] Evans M R, Juhász R and Santen L 2003 Shock formation in an exclusion process with creation and annihilation *Phys. Rev. E* **68**(2) 026117
- [45] Ezaki T and Nishinari K 2012 Exact stationary distribution of an asymmetric simple exclusion process with langmuir kinetics and memory reservoirs *J. Phys. A: Math. Theor.* **45** 185002
- [46] Sato J and Nishinari K 2016 Relaxation dynamics of the asymmetric simple exclusion process with langmuir kinetics on a ring *Phys. Rev. E* **93**(4) 042113
- [47] Sato J and Nishinari K 2018 Relaxation dynamics of closed diffusive systems with infinitesimal langmuir kinetics *Phys. Rev. E* **97**(3) 032135
- [48] Yamamoto H, Ichiki S, Yanagisawa D and Nishinari K 2022 Two-lane totally asymmetric simple exclusion process with extended langmuir kinetics *Phys. Rev. E* **105**(1) 014128
- [49] Dhiman I and Gupta A K 2016 Origin and dynamics of a bottleneck-induced shock in a two-channel exclusion process *Phys. Lett. A* **380** 2038–2044 ISSN 0375-9601
- [50] Verma A K, Gupta A K and Dhiman I 2015 Phase diagrams of three-lane asymmetrically coupled exclusion process with langmuir kinetics *Europhys. Lett.* **112** 30008